Research Article



Multichannel sequential display LED driver with optimal transient performance and efficiency via synchronous integral control

ISSN 1755-4535 Received on 30th January 2020 Revised 20th May 2020 Accepted on 23rd June 2020 E-First on 3rd August 2020 doi: 10.1049/iet-pel.2020.0128 www.ietdl.org

Haifeng Wang¹ ⋈, Tingshu Hu²

¹Electro-Mechanical Engineering, Penn State University New Kensington, 3550 Seventh Street Road, New Kensington, PA, USA ²Electrical & Computer Engineering, UMASS Lowell, 220 Pawtucket St, Lowell, MA, USA ⊠ E-mail: hzw87@psu.edu

Abstract: This study proposes a high performance multichannel sequential display light emitting diode (LED) driver with pulse width modulated dimming control. A synchronous integral control strategy is developed for achieving optimal transient performances for the channel voltages and ideal rectangular waveforms for the LED current, which will help to maintain high efficiency and extend the lifetime of the LEDs. By synchronous integral control, each channel has a corresponding integrator whose input and output are turned on and off synchronously with the LED string. The proposed driver topology and control strategy are supported by detailed analysis on stability and transient response during on-time interval of a channel by using the averaged state-space model. The effectiveness of the design method is demonstrated with simulation. A three-channel LED driver is constructed to experimentally validate the high efficiency and high performance of the proposed topology and control strategy with desired LED current waveform and nearly constant channel voltages.

1 Introduction

Light emitting diodes (LEDs) are poised to replace traditional light sources due to their many benefits: efficiency, longevity, safety, durability, colour options and earth friendly characteristics. They are widely used for residential lighting, automotive, transportation, broadcasting and entertainment. LED technology has been continuously advanced in recent years in terms of high power, high current and high brightness. Meanwhile, highly efficient and intelligent LED drivers have been developed to bring out the best performances of LEDs by using advanced power electronics and control systems technologies.

For the purpose of saving energy or offering variable contrast, dimming controls are usually applied to LED strings to regulate the lighting level. There are basically two approaches for dimming control. One is the amplitude modulation approach, which is obtained by modulating the LED current to a desired constant level by using a linear regulator. Another one is the pulse width modulated (PWM) approach, which is obtained by periodically switching on and off a LED string, so that the average of the LED current and the brightness are adjusted by the duty cycle of the PWM signal. The PWM approach for dimming is preferred in many applications due to its high efficiency and smaller chromaticity deviation [1]. More detailed comparison between these two dimming approaches can be found in [2].

This paper is motivated by some performance problems encountered when the PWM dimming approach is adopted. Ideally, the LED current waveform under PWM dimming should be rectangular so that the current is at the rated value during on-time interval. This would help to maintain a high efficiency since the driver circuit can be optimised in terms of efficiency for the operation under rated values. Moreover, a constant rated current during on-time interval would guarantee a long lifespan of LEDs. A rectangular LED current also allows precise control of the intensity since the average current is proportional to the dimming ratio. However, the actual LED current waveforms generated by many existing PWM dimming approaches are not rectangular and may demonstrate various transient behaviours, such as overshoot, oscillations, or slow rise after being turned on [3-7]. Recent efforts have been devoted to improving the transient performance during the on-time interval of PWM dimming. For example, the overshoot in LED current was suppressed by using an additional integrated

soft-start circuit in [3]. An adaptive timing difference compensation strategy was developed in [8] to achieve accurate control of LED current. In [9], a dual-mode dimming control and current-balancing design was proposed for backlight applications by using a constant voltage constant current dimming scheme and a current balancing transformer. To achieve fast transient response for PWM dimming, a constant on-time controlled boost converter was proposed in [10].

In the above-mentioned works, the PWM dimming performance was improved by exploring different circuit topologies and advanced timing schemes or switching strategies. This work will take a different approach by utilising techniques for control design and optimisation. While the LED driver configuration will be derived from some existing single input multiple output (SIMO) boost converter, the main thrust is to develop a synchronous integral control strategy and cast the parameter design problem into a linear matrix inequality (LMI) based optimisation problem. With the LMI-based optimisation technique, the transient performance indices, such as overshoot and settling time, can be interpreted with matrix inequalities. As a result of the optimisation, there will be minimal transient oscillation in channel voltages and the LED current waveforms will be nearly rectangular. The effectiveness of the proposed design method is validated by simulation and experimental results, which demonstrate a 0.8% maximal deviation from the reference LED current, a significant improvement from 2.8% in [8] and 3.7% in [10].

The rest of the paper is organised as follows. The proposed multichannel LED driver with synchronous integral control will be described in Section 2. Detailed stability and transient analysis of the proposed LED driver topology and control strategy are conducted in Section 3. An experimental driver with three output channels was constructed to validate the effectiveness of the proposed control strategy, as will be demonstrated in Section 4. Conclusions are drawn in Section 5.

2 Proposed sequential display LED driver with synchronous integral control

2.1 LED driver configuration

The proposed multichannel sequential display LED driver configuration is depicted in Fig. 1. It is adapted for PWM dimming

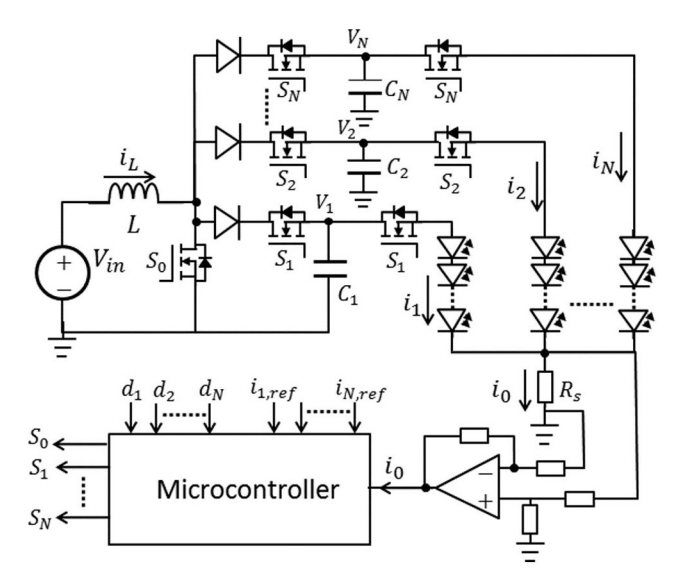


Fig. 1 Schematic of the proposed multichannel LED driver

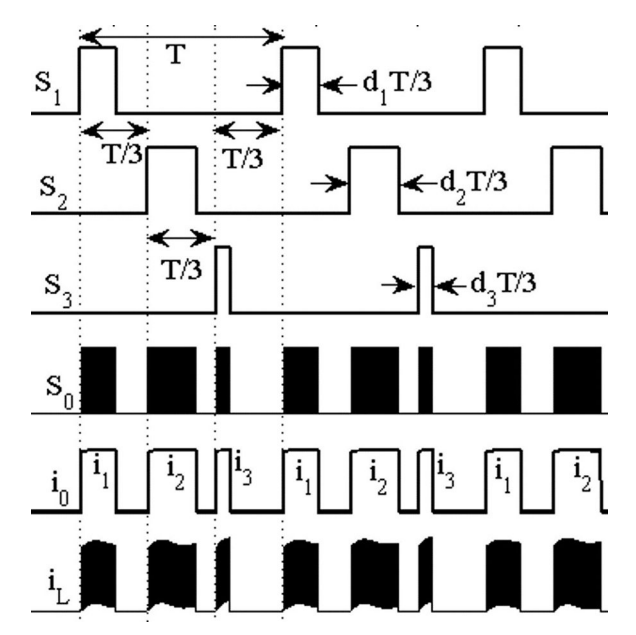


Fig. 2 Timing chart for gate signals and currents

from some existing SIMO dc-dc converters, e.g. see [11, 12]. In Fig. 1, each output voltage V_n , n=1,...,N is stabilised by a separate capacitor C_n . On both sides of the capacitor C_n are two MOSFETs, which are turned on and off simultaneously (The gates of the two simultaneous MOSFETs are connected to the same driver output via separate gate resistors.). The gate signals S_1 , S_2 , ..., S_N are generated so that only one pair of MOSFETs are allowed to be turned on at one time and the N channels take turns to operate. When N=3, this configuration and timing strategy can be applied to precision colour control in LED display panels [13] and in LED backlight driving systems [14–17], where the three primary-colour LEDs are turned on sequentially. One advantage of this sequential colour display scheme is the reduction of power consumption by removing colour filter [14, 16].

In each channel, the MOSFET to the right of C_n turns on and off the LED string. The left-hand-side MOSFET and the series diode ensure that there is no current flow between the channels and that the capacitor voltage V_n does not change when the corresponding LED string is turned off. Due to the anti-parallel body diode in the MOSFETs, the diodes are necessary to allow for different channel voltages. As observed from experiments, the channel voltages can be different by nearly 1 V when the channels have different dimming ratios. The channel with higher dimming ratio requires lower voltage due to the temperature dependent I-V curve of the LEDs. Since the channels operate alternatively, they

are joined together and connected to a single current sense resistor R_s , which will save the space and cost. Moreover, more current sensors result in increased power loss.

Similar SIMO boost converter topology was adopted in [8] for an LED driver for display backlight applications. A distinctive difference is that there is an additional MOSFET on the right-hand-side of the filter capacitor for each channel. This ensures that the LED strings are turned on alternatively and that each capacitor voltage is maintained at a constant value when that channel is turned off, which is crucial not only for minimising voltage oscillation but also for achieving ideal rectangular current waveform for each LED string with PWM dimming.

Fig. 2 illustrates the timing of the gate signals, and some typical inductor current i_L and output current i_0 (generated by simulation). Suppose that there are three channels. The period T of one dimming cycle is divided equally into three sub-intervals. The nth channel operates only during the nth subinterval and the on-time is modulated by the dimming ratio $d_n \in [0, 1)$. Thus, the on-time for the nth channel over one period is $d_n T/3$ and the actual duty ratio is $d_n/3$. During the on-time of the nth channel, the circuit behaves like a typical single output boost converter, with its output voltage V_n and current i_0 controlled by the duty cycle of the gate signal S_0 . Since the switching frequency of S_0 is much higher than 1/T, its plot is a black rectangular when one channel is on. The output current i_0 is the sum of the channel currents. Each channel current i_0 can be extracted from i_0 by using the gate signal S_n .

The dimming is achieved by changing $d_1, d_2, ..., d_N$ between 0 and 1. Ideally, the LED current i_n for each string should be the rated value when this string is turned on. Thus, the ideal waveform of i_n is rectangular with frequency 1/T and duty ratio d_n/N .

For high efficiency, the inductor current i_L should be 0 when all channels are turned off. This is achieved by setting S_0 at 0 when all channels are off, and choosing circuit parameters so that i_L is at discontinuous conduction mode (DCM) or near DCM during the interval when one channel is on. Fig. 2 shows the case where i_L is at the continuous conduction mode but very close to DCM when one channel is on. To avoid cross-regulation between the channels, a dead time should be implemented between the turning off of one channel and the turning on of another channel. To ensure safe switching and to protect the MOSFETs, especially S_0 , the signals S_1 , S_2 , S_3 should be turned off after S_0 is turned off, by a few switching periods.

2.2 Synchronous integral control

The control objective is to maintain a desired LED string current $i_{n,\text{ref}}$ for each channel during its on-time. Ideally, the output voltage V_n is maintained at a constant desired value, so that when the nth channel is turned on, a rated current flows through this LED string. As this channel is turned on and off by a PWM signal, the LED current has an ideal rectangular waveform.

The voltage control was used in some literature but has some disadvantages, since the I–V curve of the LEDs is not fixed. It depends on the temperature and may vary with ageing [18]. For example, with a constant voltage supply, as the operation time increases, the current increases since the equivalent series resistance decreases due to increasing junction temperature [5]. As observed in the experiment, as the dimming ratio is increased, the LED string's voltage needs to be decreased to maintain a desired current. This is due to the reduction of the forward voltage and the equivalent series resistance as the temperature increases. Thus, it is preferred to control the LED current directly so that it follows a desired rectangular reference. For this purpose, the LED current is sensed by R_s .

Recall that when all LED strings are off, the inductor current is 0 and the output voltages are kept as constants. After one string is turned on, the transience will cause the corresponding voltage V_n to temporarily decrease then go back to a steady-state value after some oscillation. To produce a nearly rectangular waveform for the LED current, the feedback control should be designed to achieve

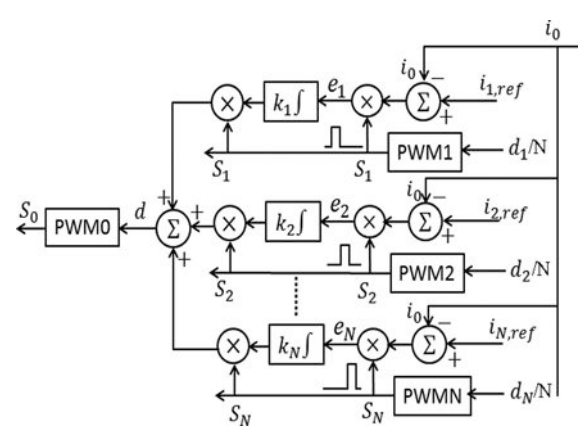


Fig. 3 Schematic of the synchronous integral control

fast transience with minimal oscillation during the on-time interval for each channel.

It was shown in [19, 20] that a simple integral control can achieve practically global stability for general dc–dc converters. For a boost converter with multiple channels which take turns to operate, this paper proposes a control scheme with synchronous integral control, as depicted in Fig. 3. The inputs to the controller are $i_0, i_{1,\text{ref}}, \ldots, i_{N,\text{ref}}$ and d_1, d_2, \ldots, d_N . The reference currents $i_{n,\text{ref}}$ can be set as constants (such as the rated values) in the controller to reduce the number of inputs. The outputs are the gate drive signals S_0, S_1, \ldots, S_N . The gate signals S_1 to S_N are modulated by d_1/N to d_N/N , with the same dimming frequency 1/T and a phase delay of T/N between S_n and S_{n+1} . The dimming ratios d_n are <1 so that only one channel is turned on at a time. The gate drive signal S_0 for the boost converter is modulated by duty ratio d with a much higher frequency. The proposed control scheme will be implemented by a micro-controller.

Each channel has an integrator whose input and output are turned on and off at the same time by the corresponding gate signal S_n , which is implemented by multiplying 1 or 0, hence the name – synchronous integral control. The synchronous input for the integrator allows only the tracking error for the corresponding channel to be integrated. Hence, during the off time of one channel, the output of the integrator stays a constant, which is crucial for achieving optimal transient response for the next on-time interval. The synchronous output of the integrators allows only one integrator output to be passed to the input of PWM0, as the duty ratio d for S_0 .

With the proposed driver topology and synchronous integral control, the whole feedback system behaves like a single input single output boost converter with integral control during the ontime interval for each channel. The transient behaviour during each on-time interval is determined by the initial values (at the beginning of each on-time interval) of the integrator output, the capacitor voltage V_n , the integral gain k_n and the circuit parameters L and C_n . It also depends on the parameters of the switching devices and LEDs, which will be assumed to be given.

As will be clear in the next section, the proposed driver topology and the synchronous integral control scheme provide an ideal framework for achieving desired transient performance with good initial conditions on integrator output and capacitor voltage. The rest task is to design integral gains k_n and circuit parameters L and C_n for further improvement of the transient response.

3 Control design for stability and optimal transient response

3.1 Stability and transient analysis via state-space description

As explained in the previous section, the ideal rectangular waveforms for the LED currents require a control design which yields a fast transient response with minimal oscillations during the on-time interval for each channel. In this section, the averaged

state-space model will be used to analyse the stability and transient response of the proposed LED driver with synchronous integral control. The topology of the driver and the control scheme make the whole system behave like a typical single input single output boost converter during the on-time interval of each channel. For illustration, the following analysis will be conducted on channel 1. The other channels have the same structure but the parameters can be different.

To avoid confusion, the high switching frequency of S_0 is denoted as f_0 (in the range of a few hundred kHz) and the low switching frequency of S_1 as f_1 (a few hundred Hz). For simplicity of notation, v_1 and i_L denote the averaged capacitor voltage V_1 and inductor current (averaged with respect to the switching period of S_0). Recall that the control input for the boost converter is the switching duty cycle d for S_0 .

Assume that a steady periodic waveform (with respect to the dimming frequency f_1) has been formed, so that a desired LED current $i_{1,\text{ref}}$ is reached before the LED string is turned off for one period. Let the corresponding steady-state values for v_1 , i_L and d be $v_{1,\text{ss}}$, $i_{L,\text{ss}}$ and d_{ss} , respectively. With the integral control, the closed-loop system has three state variables: the inductor current i_L , the capacitor voltage v and the output of the channel 1 integrator, which is the duty ratio d. Note that the outputs of other channels' integrators are turned off when channel 1 is on.

Let the time when channel 1 is turned on (the rising edge of S_1 in Fig. 2) be t=0. By the proposed topology of the LED driver, the capacitor voltage v_1 is kept unchanged during the off-time interval of channel 1. Thus, $v_1(0) = v_{1.ss}$. By the synchronous integral control scheme, the output of channel 1's integrator is also kept at the value before it is turned off last time, which is d_{ss} . Thus, $d(0) = d_{ss}$. By the design of the LED driver, the inductor current i_L is 0 when all channels are turned off, so $i_L(0) = 0$. Hence, for the state vector

$$\begin{bmatrix} i_L(0) \\ v_1(0) \\ d(0) \end{bmatrix} = \begin{bmatrix} 0 \\ v_{1,ss} \\ d_{ss} \end{bmatrix}$$
 (1)

To study the transient response, the deviation of the state variables from the steady-state values (with respect to the on-time interval) should be examined. Denote the deviation variables as

$$\Delta i_L = i_L - i_{L,ss}, \Delta v_1 = v_1 - v_{1,ss}, \Delta d = d - d_{ss}$$
 (2)

Define the new state as x

$$x = \begin{bmatrix} x_1 \\ x_2 \\ x_3 \end{bmatrix} = \begin{bmatrix} \Delta i_L \\ \Delta v_1 \\ \Delta d \end{bmatrix}$$
 (3)

Then the initial condition for the new state x is

$$x(0) = \begin{bmatrix} -i_{L \text{ ss}} & 0 & 0 \end{bmatrix}^{\mathrm{T}} \tag{4}$$

which means that two of the three state variables are already at the steady-state values. This is ensured by the proposed LED driver topology and control scheme, which is crucial for good transient performance. Only the inductor current is away from the steady-state value. This cannot be changed since it is necessary to keep the inductor current 0 when all channels are off, so that high efficiency can be ensured.

It is clear that the transient response is caused by the deviation of the inductor current from its steady-state value. In what follows, the relationship between the transient response and the design parameters, including the integral gain k_1 , the inductance L and the capacitance C_1 , will be studied. Based on this relationship, the parameters can be selected for the optimal transient performance.

Let the total equivalent series resistance of the LED string (including R_s and the on-resistance of the MOSFET) be R_{led} and let the forward voltage drop be v_F

$$v_1 = v_F + R_{\text{led}} * i_1 \tag{5}$$

At steady state

$$v_{1,ss} = v_F + R_{led} * i_{1,ref}$$
 (6)

It follows that

$$i_1 - i_{1,\text{ref}} = \frac{v_1 - v_{1,\text{SS}}}{R_{\text{led}}} = \frac{x_2}{R_{\text{led}}}$$
 (7)

By the integral control

$$\Delta d = -k_1 \int (i_1 - i_{1,\text{ref}}) dt \tag{8}$$

which gives

$$x_3 = \Delta d = -\frac{k_1}{R_{\text{led}}} \int (v_1 - v_{1, ss}) dt = -\frac{k_1}{R_{\text{led}}} \int_0^x dt$$
 (9)

This yields

$$\dot{x}_3 = -\frac{k_1}{R_{led}} x_2 \tag{10}$$

By using the state-space averaged method [21], the differential equations for x_1 and x_2 can be derived. To examine the transient response, the parasitic series resistances of the boost converter should be taken into account. Ignoring these resistances will yield stronger oscillation and larger overshoots/undershoots for the transient responses. Let the equivalent series resistance for the inductor, the MOSFET and the diode be R_L , $R_{\rm on}$, R_d , respectively (The capacitor's ESR is not considered here since it is very small as compared with $R_{\rm led}$. Its effect on the LED current is negligible, but will substantially complicate the state matrices). Recall that for the LED string, the total forward voltage drop is $v_{\rm F}$ and the equivalent series resistance is $R_{\rm led}$. Define the following matrices:

$$\boldsymbol{K}_{0} = \begin{bmatrix} \frac{1}{L} & 0\\ 0 & \frac{1}{C_{1}} \end{bmatrix}, \boldsymbol{B}_{1} = \begin{bmatrix} 1 & 0\\ 0 & \frac{1}{R_{\text{led}}} \end{bmatrix}$$
(11)

$$A_{1} = \begin{bmatrix} -(R_{L} + R_{\text{on}}) & 0\\ 0 & \frac{-1}{R_{\text{led}}} \end{bmatrix}$$
 (12)

$$A_{2} = \begin{bmatrix} -(R_{L} + R_{d} + R_{\text{on}}) & -1\\ 1 & \frac{-1}{R_{\text{led}}} \end{bmatrix}$$
 (13)

The averaged state-space equation for i_L and v_1 can be derived from circuit laws as follows:

$$\begin{bmatrix} \frac{\mathrm{d}i_L}{\mathrm{d}t} \\ \frac{\mathrm{d}v_1}{\mathrm{d}t} \end{bmatrix} = \mathbf{K}_0 (d\mathbf{A}_1 + (1-d)\mathbf{A}_2) \begin{bmatrix} i_L \\ v_1 \end{bmatrix} + \mathbf{K}_0 \mathbf{B}_1 \begin{bmatrix} v_{\mathrm{in}} \\ v_{\mathrm{F}} \end{bmatrix}$$
(14)

At steady state, the left hand side is 0. It follows that

$$\begin{bmatrix} i_{L,ss} \\ v_{1,ss} \end{bmatrix} = -(d_{ss} \mathbf{A}_1 + (1 - d_{ss}) \mathbf{A}_2)^{-1} \mathbf{B}_1 \begin{bmatrix} v_{in} \\ v_F \end{bmatrix}$$
 (15)

It is clear to see that the steady-state values $i_{L,ss}$ and $v_{1,ss}$ are independent of the parameters L and C_1 . Define

$$\mathbf{A}_0 = d_{ss}\mathbf{A}_1 + (1 - d_{ss})\mathbf{A}_2, \ \mathbf{B}_0 = (\mathbf{A}_1 - \mathbf{A}_2) \begin{bmatrix} i_{L,ss} \\ v_{1,ss} \end{bmatrix}$$
 (16)

Then a small-signal model for x_1 and x_2 can be derived as follows:

$$\begin{bmatrix} \dot{x}_1 \\ \dot{x}_2 \end{bmatrix} = \boldsymbol{K}_0 \boldsymbol{A}_0 \begin{bmatrix} x_1 \\ x_2 \end{bmatrix} + \boldsymbol{K}_0 \boldsymbol{B}_0 x_3 \tag{17}$$

Denote

$$\mathbf{K} = \begin{bmatrix} \mathbf{K}_0 & 0 \\ 0 & k_1 \end{bmatrix} = \begin{bmatrix} 1/L & 0 & 0 \\ 0 & 1/C_1 & 0 \\ 0 & 0 & k_1 \end{bmatrix}, \tag{18}$$

$$\mathbf{A} = \begin{bmatrix} \mathbf{A}_0 & \mathbf{B}_0 \\ 0 & -\frac{1}{R_{\text{ted}}} \end{bmatrix} \quad 0$$
 (19)

Combining (10) and (17), the closed-loop state equation for x is

$$\dot{x} = KAx \tag{20}$$

Here the positive diagonal matrix K contains all the three design parameters L, C_1 and k_1 , and the matrix A contains other given circuit parameters. This well separated structure of the system matrix KA will facilitate the design of L, C_1 and k_1 for stability and optimal transient responses. The system is stable if all eigenvalues of KA have negative real parts.

After channel 1 is turned on, the transient response for the closed-loop system is

$$x(t) = e^{KAt}x(0) (21)$$

$$x(0) = \begin{bmatrix} -i_{L.SS} \\ 0 \\ 0 \end{bmatrix} \tag{22}$$

To achieve desirable transient response with ideal LED current waveform, the deviation of the capacitor voltage, which is $v_1 - v_{1,ss} = x_2$, should be as small as possible. Furthermore, a steady state should be almost reached by the time this channel is turned off for one period. Denote $C_s = [010]$, then

$$x_2(t) = C_s x(t) = C_s e^{KAt} x(0)$$
 (23)

Denote t_s as the settling time, which is the time required for x(t) to converge within 5% of x(0). Then the design objective is to choose

a positive diagonal matrix K so that the maximal value of $x_2(t)$ is minimised, while the settling time t_s is less than a prescribed limit. This objective can be addressed by using the method developed in [22], which is discussed in more detail in the next section.

3.2 Design objective and parameter optimisation

The objective of minimising the maximal value of $x_2(t)$ by choosing the three design parameters L, C_1 , k_1 can be converted into a LMI based optimisation problem. The main idea is to use an invariant ellipsoid to bound the transient response $x(t) = e^{KAt}x(0)$ and evaluate the maximal value of $x_2(t)$ via this invariant ellipsoid. Similar problems have been addressed in [22]. The requirement on the settling time t_s can also be imposed via a matrix inequality. With the treatment in [22], the optimisation problem can be formulated as follows:

$$\inf_{P>0, K>0} \gamma \tag{24}$$

$$PKA + A^{\mathrm{T}}KP \le -\beta_0 P \tag{25}$$

$$x(0)^{\mathsf{T}} \boldsymbol{P} x(0) \le 1 \tag{26}$$

$$C_s^{\mathrm{T}}C_s \le \gamma^2 \mathbf{P} \tag{27}$$

$$K_1 \le K \le K_2 \tag{28}$$

In the above optimisation problem, β_0 is a given positive number corresponding to the prescribed limit of settling time. If (25) is satisfied, the closed-loop system will be stable and the settling time will be less than $-2\log 0.05/\beta_0$. When all the constraints (25)–(27) are satisfied, γ will be an upper bound for the maximal deviation $|x_2(t)| = |C_sx(t)|$.

The optimisation problem has two matrix variables, a positive definite matrix P and a positive diagonal matrix K. Recall that K contains the design parameters L, C_1 , k_1 . The additional constraint (28) imposes a range for each parameter so that other requirements can be satisfied, such as the ripple size of inductor current and output voltage.

The optimisation problem (24) contains a bilinear matrix inequality (BMI) (25). The standard treatment of BMI problems is to use an iterative method by optimising each matrix variable alternatively. The algorithm can be summarised as follows.

Algorithm to solve optimisation problem (24):

Step 1: Form all the constants, A, β_0 , x(0), C_s , K_1 , K_2

Step 2: Choose an initial variable K so that KA is stable

Step 3: Solve (24) for P, γ , with a fixed K using LMI toolbox

Step 4: With P obtained from step 3, find K to produce the maximal gap in (25), in order to create more design freedom for P in the next round. This can be done by randomly generating a positive definite matrix Q, (i.e. R = rand(3), Q = R'R). Then optimise K using LMI toolbox so that the inequality below

$$PKA + A^{\mathrm{T}}K P \le -\beta_0 P - \eta Q \tag{29}$$

is satisfied with the maximal η .

Step 5: If η is greater than a threshold, i.e. 10^{-8} , go back to Step 3 and repeat the iteration. If η is less than the threshold, then terminate the algorithm.

For easy reference, the Matlab source code for the above algorithm is included in Fig. 4.

3.3 Design example

In this section, the effectiveness of the control design method will be demonstrated with one example. The parameters for an experimental circuit are used for the computation. The source voltage is $V_{\rm in}=8\,{\rm V}$. Assume that all LED strings have the same

parameters. For each string, the forward voltage and ESR are $v_{\rm F}=10\,{\rm V}$ and $R_{\rm led}=10.4\,\Omega$, respectively. The on-resistance of all MOSFETs is $R_{\rm on}=0.07\,\Omega$. The on-resistance of all diodes is $R_d=0.2\,\Omega$. The ESR of the inductor is $R_L=0.03\,\Omega$. The reference current is set at $i_{\rm 1,ref}=0.25\,{\rm A}$.

The values for some variables at the desired steady state are computed as follows. To generate a desired LED current $i_1 = i_{1,ref} = 0.25 \text{ A}$, it is required that $v_1 = v_F + R_{\text{led}}i_1 = 12.6 \text{ V}$. The corresponding steady-state values for other variables (for the ontime interval) can be computed via (15) by iterating on d_{SS} , which are $i_{L,\text{SS}} = 0.4016 \text{ A}$, $v_{1,\text{SS}} = 12.6 \text{ V}$, $d_{\text{SS}} = 0.375$. Based on these values and circuit parameters, the matrix A in (19) can be computed. The initial condition when the LED string is turned on is $x(0) = [-0.401600]^T$.

To set up the optimisation problem (24), the values for β_0 and K_1, K_2 are needed. Recall that the settling time $t_s < -2\log(0.05)/\beta_0$ s. The requirement on t_s depends on the dimming frequency and the number of channels. Suppose that the dimming frequency is 200 Hz and there are three channels. It is required that the settling time be less than the on-time of one channel for 0.5 dimming ratio. This gives $t_s < 0.5/200/3$ s and $\beta_0 \simeq 7000$. The lower and upper bounds K_1 , K_2 on K depends on the range of L and C_1 to satisfy certain requirement on ripple, e.g. $L \in [5,20]\mu H$ and $C_1 \in [20,200]\mu F$. There is no specific requirement on the integrator gain k_1 except for stability, which is ensured by (25).

By using the algorithm in the previous section, the parameters are determined as $L=5\,\mu\mathrm{H}$, $C_1=191\,\mu\mathrm{F}$ and $k_1=1465$. By using these parameters, the transient response of the LED current i_1 is computed by using (21) and $i_1(t)=i_{1,\mathrm{ref}}+x_2(t)/R_{\mathrm{led}}$, which is plotted in Fig. 5a. The left-hand-side plot shows the full scale and the right-hand-side plot shows details of the oscillation around the steady-state value. It can be seen that the maximal LED current deviation from the reference value is <2 mA, which is about 0.8% of the reference current 250 mA. This is a significant improvement as compared to the results reported in the literature. The LED current deviation reported in [8, 10] is 2.8 and 3.7%, respectively. To show the effect of optimisation, the deviations of capacitor voltage are compared in Fig. 5b with optimised and non-optimised design parameters.

4 Experimental result

An experimental driver circuit with three channels of outputs was constructed (see Fig. 6) using the proposed configuration in Fig. 1. Three strings of LEDs were connected to the outputs. Each string had four LEDs in series. Same LEDs were used for all strings so their total forward voltage and ESR were assumed to be the same.

The parameters of the LEDs and switching devices were used in the control design to select the optimal inductance L, capacitance C_1 , C_2 , C_3 and integrator gains k_1 , k_2 , k_3 . Since the LED strings were assumed to be symmetric, same capacitance and integrator gain were used for all channels. For easy reference, the circuit parameters and controller parameters are listed in Table 1.

The synchronous integral control proposed in Fig. 3 was implemented by Texas Instrument's TMS320F28335. The experiment was conducted under room temperature (25°C). The reference currents for the three channels were set at the same value: $i_{n,\text{ref}} = 0.25 \text{ A}$, n = 1, 2, 3. The dimming ratio for each channel was varied between 10 and 90%.

Fig. 7 shows the experimental results when all three dimming ratios were set at 50%. Three channel voltages V_1 , V_2 , V_3 and the output current i_0 were recorded. To increase the signal-to-noise ratio, the current was scaled by 10 before fed to the microcontroller. The three channel voltages were nearly flat, with periodic noisy intervals, which occurred when that channel was turned on.

The output current $(10i_0)$ is at the bottom of Fig. 7. Although i_0 is the total current of all channels, it is easy to tell which channel is on from the noisy voltage intervals above the current waveform. On the right-hand-side pane of the figure are some measurements of the channel voltages and output current. The three channel

voltages were all equal to 12.2 V, indicating that the three LED strings are nearly symmetric. The current i_0 's nearly rectangular waveform demonstrates ideal transient response during the on-time of each channel. The tracking performance of the reference was also satisfactory except for measurement noise and switching ripples.

Fig. 8 shows the waveforms for $d_1 = 80\%$, $d_2 = 40\%$ and $d_3 = 20\%$. Fig. 9 shows those for $d_1 = 90\%$, $d_2 = 40\%$ and $d_3 = 10\%$. The same reference currents were used for all channels. Both cases demonstrate nearly rectangular waveforms for the current, even for 10% dimming ratio. The channel voltages are also nearly flat. However, the values for the channel voltages visibly changed with the dimming ratio for channel 1 and channel 3, as seen from the right-hand-side pane of each figure. For channel 1, the voltage decreased as the dimming ratio was increased. For channel 3, the

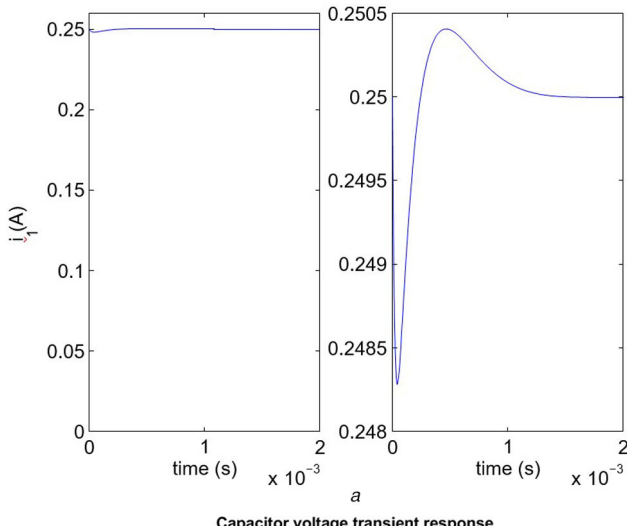
```
%Step 1
%Initial design parameters
L0=10e-6;C0=100e-6;k0=800;
%Other parameters
Vin=8;d0=0.375;RF=2.6*4; RL=0.1;
Ron=0.07;Rd=0.2;vF=2.5*4;
%Set initial design parameters
L=L0;C=C0;k=k0;
%Form matrices
A1=[-(RL+Ron)/L 0;0-1/RF/C];
A2=[-(RL+Rd+Ron)/L-1/L;1/C-1/RF/C];
B1=[1/L 0;0 1/RF/C];
A0=(A1*d0+(1-d0)*A2);
E=[Vin;vF];
x00 = -inv(A0)*B1*E;
iled = (x00(2)-vF)/RF;
B=(A1-A2)*x00;
AL=[A0 B; 0 - k/RF 0];
x0=[-x00(1);-0;-0.00];
C1=[0\ 1\ 0];
%Step 2, Set initial K for iteration
K=[2 0 0;0 0.55 0;0 0 1.8];
Gap=1;
while Gap > 1e-8
%Step 3
% Find optimal P and gamma
setlmis([])
  beta = lmivar(1,[1,1]);
  P = lmivar(1,[3,1]);
  lmiterm([-1 1 1 P],1,1)
  lmiterm([1 1 1 0],eye(3)*1e-9) %P>0
  lmiterm([2 1 1 P],1,K*AL,'s')
  lmiterm([-2 1 1 P],-1,7000) % (25)
  lmiterm([3 1 1 P],x0',x0)
  lmiterm([-3 1 1 0],1) % (26)
```

Fig. 4 Matlab source code for solving the optimisation problem (24)

voltage increased as the dimming ratio was decreased. Since the LED currents were maintained as the same reference value under integral control, the increase of V_3 must be caused by the increase of the forward voltage drop or the increase of the ESR in channel 3. Similarly, the decrease of V_1 must be caused by the decrease of forward voltage or the decrease of ESR in channel 1. All these results can be explained as the effect of temperature. It should be noted that all the figures were recorded after the measurement readings had reached steady states, which took about 5–10 min after the beginning of a test.

These results confirm the necessity of using current control in LED drivers with dimming functions. If a voltage control is implemented for the channel output, the LED string current will fluctuate around the rated value, causing colour shift or damaging the LEDs.

```
lmiterm([-4 1 1 P].1.1)
  lmiterm([4 1 1 beta],C1'*C1,1) %(27)
  lmisys=getlmis;
  c=[-1 zeros(1.6)];
  op=[0.0000001 300 1e15 16 1];
  [t,X]=mincx(lmisys,c,op);
% Extract optimal gamma and P
  beta=-t;
  gamma = sqrt(1/beta);
  P=dec2mat(lmisys,X,P);
% Step 4: Find K to create max gap
  R=randn(3);Q=R'*R;
  setlmis([])
  eta=lmivar(1,[1,1]);
  K= lmivar(1,[1,1;1 1;1 1]);
  lmiterm([1 1 1 K],1,1)
  lmiterm([-1 1 1 0],[2 0 0;0 5 0;0 0 10])
  lmiterm([-2 1 1 K],1,1) % K1 < K
  lmiterm([2 1 1 0],[0.25 0 0;0 0.3 0;0 0 0.1])
  lmiterm([3 1 1 K],P,AL,'s') % (29)
  lmiterm([-3 1 1 0],-7000*P)
  lmiterm([-3 1 1 eta],-Q,1)
  lmisys=getlmis;
  c=[-1 zeros(1,3)];
  op=[0.0000001 300 1e15 16 1];
  [t,X]=mincx(lmisys,c,op);
 %extract optimal eta and K
  eta=dec2mat(lmisys,X,eta);
  K=dec2mat(lmisys,X,K);
  Gap=eta;
end
 % Final design parameters
 L=L0/K(1,1);
 C=C0/K(2,2);
 k=k0*K(3,3);
```



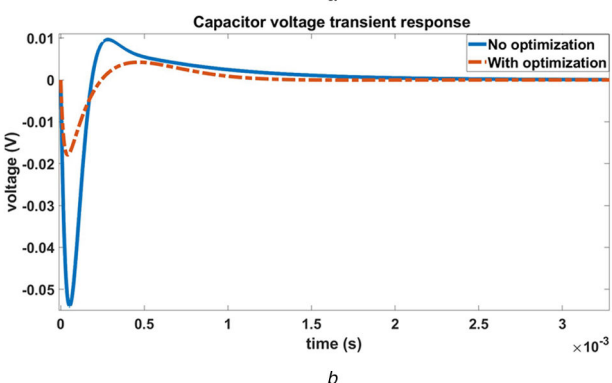


Fig. 5 Comparison of the transient response with optimised and non-optimised design parameters

(a) Transient response of LED current i_1 , (b) Transient variation of LED channel 1 voltage

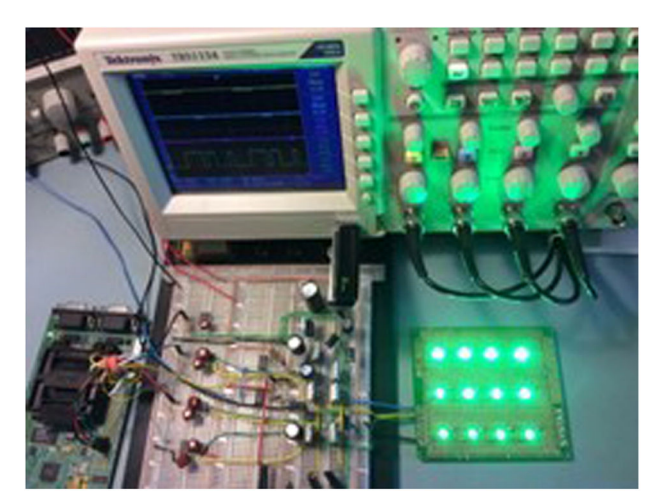


Fig. 6 Photograph of the LED driver prototype and experiment setup

When the LED driver is applied to sequential RGB display, the rated currents for the LED strings may be different [23, 24]. Fig. 10 shows the waveforms when different reference currents were set for the channels: $i_{1,\text{ref}} = 0.1 \,\text{A}$, $i_{2,\text{ref}} = 0.15 \,\text{A}$ and $i_{3,\text{ref}} = 0.25 \,\text{A}$. The output current i_0 waveform had three levels and each level was nearly rectangular. Also note that the channel voltages are visibly different.

The efficiency of the driver circuit was computed from measurements of the average current of the power supply, the actual input voltage, the output voltage and the average LED current. Due to the temperature-dependent I–V curve of the LEDs [25–28], it takes about 5–10 min for the readings to reach steady-state values, after the beginning of each test. Fig. 11 plots the efficiency versus the dimming ratio d_n . Here the same dimming

Table 1 Circuit and controller parameters

Symbol	Description	Quantity	Unit
V _{in}	supply voltage	8	[V]
L	inductance	5	[µ H]
R_L	inductor ESR	0.03	[Ω]
Ron	MOSFET on-resistance	0.07	[Ω]
R_d	diode on-resistance	0.2	[Ω]
C_1, \ldots, C_N	output capacitance	200	[μ F]
R _s	current sense resistance	0.1	[Ω]
V_{F}	LED string fwd volt.	10	[V]
R _{led}	LED string ESR	10.4	[Ω]
k_1, \ldots, k_N	integrator gains	1460	_
f_0	switching frequency	330 k	[Hz]
<i>f</i> ₁	LED dimming frequency	214	[Hz]

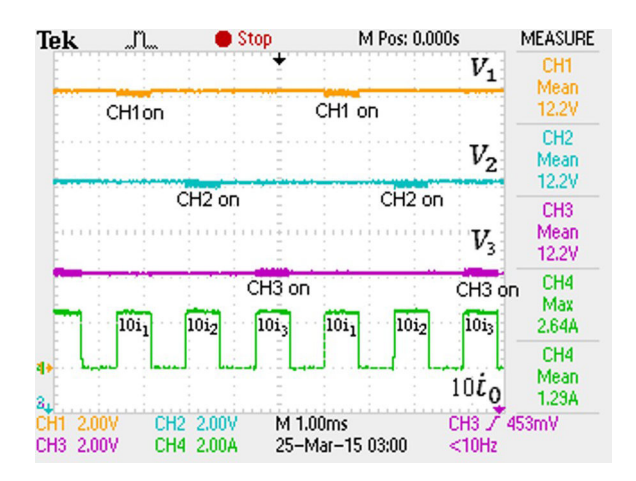


Fig. 7 Experimental waveforms for $d_1 = d_2 = d_3 = 50\%$

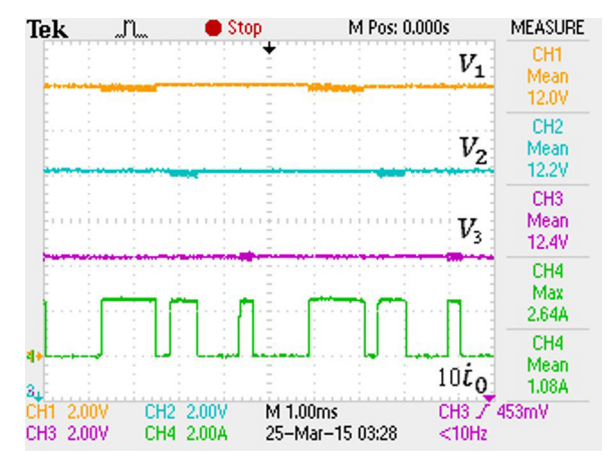


Fig. 8 Experimental waveforms for $d_1 = 80\%$, $d_2 = 40\%$, $d_3 = 20\%$

ratio was set for all channels. Recall that the actual duty ratio for channel n is d/3. The maximal efficiency was about 95.5%, which was reached at about 80% dimming ratio. For all dimming ratio between 10 and 90%, the efficiency was above 92%. The more these LEDs are dimmed, the less efficient they will be, which was also proved by the research in [29]. It is believed that the high efficiency of the driver circuit is a consequence of the more desirable transient performance with nearly rectangular current waveform and constant channel voltages than that of traditional LED drivers.

5 Conclusion

This paper proposed an LED driver and control strategy for multiple strings of LEDs with dimming functions. A synchronous integral control strategy was proposed for high efficiency and high

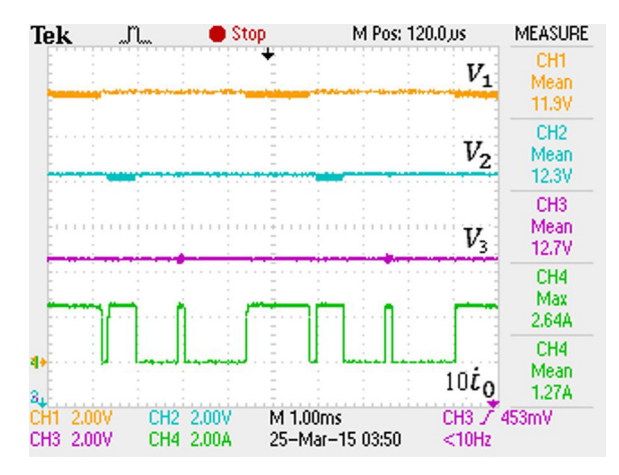


Fig. 9 Experimental waveforms for $d_1 = 90\%$, $d_2 = 40\%$, $d_3 = 10\%$

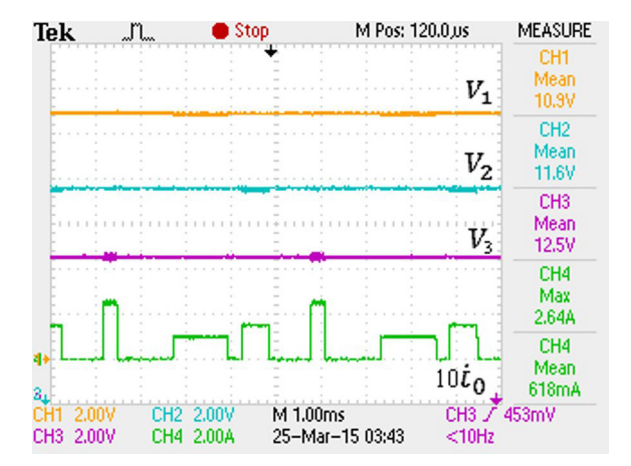


Fig. 10 Waveforms for different reference currents

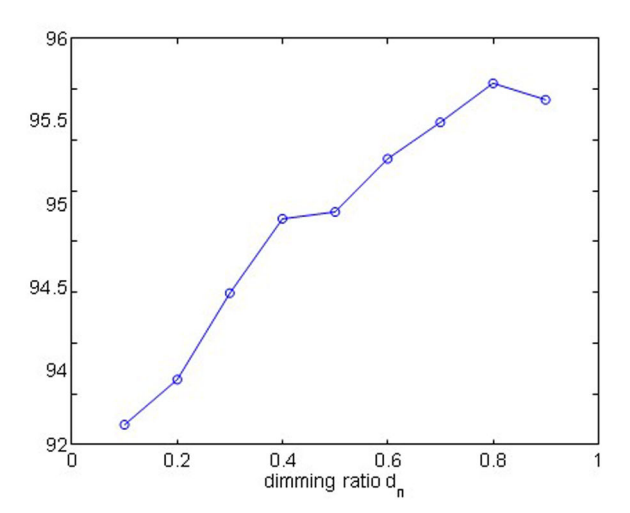


Fig. 11 Efficiency versus dimming ratio

performance LED dimming by using an integral control which is synchronous with the switching of dimming control for each channel. The control scheme is designed so that each channel's output voltage and the integrator output are kept as constants during the LED string's off-time interval. The proposed driver with PWM dimming and synchronous integral control may find applications in colour sequential display to further reduce power consumption and to achieve high colour precision.

6 Acknowledgments

This work was supported in part by the National Science Foundation under grants ECCS-1200152 and the Penn State University Research and Development Grant.

References

- Dyble, M., Narendran, N., Bierman, A., et al.: 'Impact of dimming white LEDs: chromaticity shifts due to different dimming methods'. Fifth Int. Conf. on Solid State Lighting. Int. Society for Optics and Photonics, San Diego, CA, USA, 2005, vol. 5941, p. 59411H
- Loo, K.H., Lun, W.K., Tan, S.C., et al.: 'On driving techniques for LEDs: toward a generalized methodology', *IEEE Trans. Power Electron.*, 2009, 24, [2] (12), pp. 2967-2976
- Hsieh, Y.-T., Juang, Y.-Z.: 'Analysis and suppression of overcurrent in boost LED drivers', *J. Disp. Technol.*, 2013, **9**, (5), pp. 388–395 [3]
- Jane, G., Lin, Y., Chiu, H., et al.: 'Dimmable light-emitting diode driver with [4] cascaded current regulator and voltage source', IET Power Electron., 2015, 8, (77), pp. 1305-1311
- Rodrigues, W.A., Morais, L.M.F., Donoso-Garcia, P.F., et al.: 'Comparative [5] analysis of power LEDs dimming methods'. IEEE Power Electronics Conf.
- (COBEP), Brazilian, 2011, pp. 378–383 Feng, W., Lee, F.C.: 'Optimal trajectory control of LLC resonant converters [6] for soft start-up', *IEEE Trans. Power Electron.*, 2013, **29**, (3), pp. 1461–1468 Moo, C.S., Chen, Y.J., Yang, W.C.: 'An efficient driver for dimmable LED
- [7] lighting', IEEE Trans. Power Electron., 2012, 27, (11), pp. 4613-4618
- Park, D., Liu, Z., Lee, H.: 'A 40 V 10 W 93%-efficiency current-accuracy-enhanced dimmable LED driver with adaptive timing difference compensation for solid-state lighting applications', IEEE J. Solid-State
- Circuits, 2014, 49, (8), pp. 1848–1860 Lin, Y.L., Chiu, H.J., Lo, Y.K., et al.: 'LED backlight driver circuit with dual-mode dimming control and current-balancing design', *IEEE Trans. Ind.* [9] Electron., 2013, 61, (9), pp. 4632-4639
- [10] Xu, X., Wu, X.: 'High dimming ratio LED driver with fast transient boost converter'. 2008 IEEE Power Electronics Specialists Conf., Rhodes, Greece,
- 2008, pp. 4192–4195
 Kim, H.-C., Yoon, C.-S., Jeong, D.-K., et al.: 'A single-inductor, multiple-channel current-balancing LED driver for display backlight applications'. IEEE Energy Conversion Congress and Exposition (ECCE), Denver, CO, T111 USA, 2013, pp. 3448-3451
- [12] Güler, N., Irmak, E.: 'Design and application of a novel single input-multi output DC/DC converter'. 2016 IEEE Int. Conf. on Renewable Energy Research and Applications (ICRERA), Birmingham, 2016, pp. 1039–1045 Ng, S.K., Loo, K.H., Ip, S.K., et al.: 'Sequential variable bilevel driving approach suitable for use in high-color-precision LED display panels', IEEE
- [13] Trans. Ind. Electron., 2012, 59, (12), pp. 4637–4645 Chen, C.-C., Wu, C.-Y., Chen, Y.-M., et al.: 'Sequential color LED backlight
- driving system for LCD panels', IEEE Trans. Power Electron., 2007, 22, (3), pp. 919–925
- Cheng, W.-C.: 'Power minimization of LED backlight in a color sequential display'. Proc. SID05 Conf., Boston, MA, USA, 2005, pp. 1384–1387 Zhang, Y., Chen, H., Ma, D.: 'A VO-hopping reconfigurable RGB LED driver [15]
- [16] with automatic detection and predictive peak current control', IEEE J. Solid-State Circuits, 2015, 50, (5), pp. 1287-1298
- [17] Wu, C.-Y.: 'Multistring LED backlight driving system for LCD panels with color sequential display and area control', IEEE Trans. Ind. Electron., 2008,
- 55, (10), pp. 3791–3800 Choi, S., Kim, T.: 'Symmetric current-balancing circuit for LED backlight with dimming', *IEEE Trans. Ind. Electron.*, 2012, 59, (4), pp. 1698–1707 [18]
- Hu, T.: 'A nonlinear system approach to analysis and design of power electronic converters with saturation and bilinear terms', IEEE Trans. Power
- Electron., 2011, **26**, (2), pp. 399–410 Lin, H., Wang, Z.: 'Hybrid proportional-integral model predictive control [20] strategy of modular multilevel converter'. 2017 IEEE 7th Int. Conf. on Power and Energy Systems (ICPES), Toronto, ON, 2017, pp. 52–56
- Middlebrook, R.D.: 'A general unified approach to modelling switching-[21] converter power stages', Int. J. Electron., 1977, 42, pp. 521-550
- [22] Thibodeau, T., Tong, W., Hu, T.: 'Set invariance and performance analysis of linear systems via truncated ellipsoids', Automatica, 2009, 45, (9), pp. 2046-2051
- **[23]** Durrani, S.S., Ahmad, A.Z.: 'An efficient digitally controlled for RGB LED driver'. 2017 4th IEEE Int. Conf. on Engineering Technologies and Applied Sciences (ICETAS), Salmabad, 2017, pp. 1-6
- Schemes (c. 12.1), Schemes, S. 1. (Adaptive driving bus voltage and energy recycling control schemes for low-power AC–DC RGB-LED drivers', *IEEE Trans. Ind.* [24]
- Electron., 2017, **64**, (10), pp. 7741–7748

 Zhou, J., Long, X., He, J., et al.: 'Uncertainty quantification for junction temperature of automotive LED with die-attach layer microstructure', *IEEE* [25] Trans. Device Mater. Reliab., 2018, 18, (1), pp. 86-96
- Raypah, M.E., Sodipo, B.K., Devarajan, M., et al.: 'Estimation of optical power and heat-dissipation factor of low-power SMD LED as a function of injection current and ambient temperature', IEEE Trans. Electron Devices, 2016, **63**, (1), pp. 408–413
- [27] Huang, L., Liao, S., Tsou, C., et al.: 'A silicon-based LED packaging module with a temperature-dependent capacitor for constant voltage control', *IEEE Trans. Compon. Packag. Manuf. Technol.*, 2016, 6, (5), pp. 683–691
- Zhao, L.: 'Temperature-dependent efficiency droop in Gan-based blue LEDs', IEEE Electron Device Lett., 2018, 39, (4), pp. 528-531
- Hwu, K., Jiang, W.: 'Expandable two-channel LED driver with galvanic isolation and automatic current balance', IET Power Electron., 2018, 11, (5), pp. 825-833